17. Observational Cosmology

Textbook: §27.4

Co-moving coordinate as a function of redshift

Photon path has $\mathrm{d}s = 0$. Hence,

$$\int_{t_\mathrm{e}}^{t_0} \frac{c\mathrm{d}t}{R(t)} = \int_0^{\varpi} \frac{\mathrm{d}\varpi}{\sqrt{1-k\varpi^2}} = \begin{cases} \frac{1}{\sqrt{k}}\arcsin(\varpi\sqrt{k}) & (k>0) \\ \varpi & (k=0) \\ \frac{1}{\sqrt{|k|}}\mathrm{arcsinh}(\varpi\sqrt{|k|}) & (k<0) \end{cases} \tag{17.1}$$

Writing the integral over time in terms of R for $\rho_\mathrm{m} \gg \rho_\gamma$, we have

$$\int_{t_\mathrm{e}}^{t_0} \frac{c\mathrm{d}t}{R(t)} = \int_{R(t_\mathrm{e})}^{R(t_0)} \frac{c\mathrm{d}R}{R\dot{R}} = \int_{R(t_\mathrm{e})}^{R(t_0)} \frac{c\mathrm{d}R}{H_0 R^2\sqrt{\Omega_{\mathrm{M},0}/R^3 + \Omega_{k,0}/R^2 + \Omega_{\Lambda,0}}}, \tag{17.2}$$

where we used the Friedmann equation and defined $\Omega_{k,0} \equiv -kc^2/H_0^2$.

Two solutions for flat Universes:

$$k=0,\ \Omega_\mathrm{M}=1,\ \Omega_\Lambda=0 \quad \Rightarrow \quad \varpi_\mathrm{e} = \frac{2c}{H_0}\left(\sqrt{R(t_0)} - \sqrt{R(t_\mathrm{e})}\right) = \frac{2c}{H_0}\left(1 - \sqrt{\frac{1}{1+z}}\right), \tag{17.3}$$

$$k=0,\ \Omega_\mathrm{M}=0,\ \Omega_\Lambda=1 \quad \Rightarrow \quad \varpi_\mathrm{e} = \frac{c}{H_0}\left(\frac{1}{R(t_\mathrm{e})} - \frac{1}{R(t_0)}\right) = \frac{cz}{H_0}, \tag{17.4}$$

where for the last equalities we assumed $R(t_0) = 1$ and used $R(t_\mathrm{e}) = 1/(1+z)$. Note that for the latter case of a pure cosmological constant with no matter or radiation, the universe is infinitely old.

Horizon distance

With the above, we can ask for any time from what distance photons arrive that were emitted at the Big Bang. This is,

$$d_\mathrm{h}(t) = R(t)\int_0^t \frac{c\mathrm{d}t'}{R(t')} \tag{17.5}$$

For a flat, matter-dominated Universe (i.e., $\Omega_\mathrm{M}=1$, $\Omega_\Lambda=0$), one finds from the above $d_\mathrm{h}(t) = 3ct$ (using that $t = \frac{2}{3}t_H = 2/3H$).

For a flat, Λ-dominated Universe, the horizon is at infinity (though also infinitely redshifted). This is because in this model the Universe was very close together for an infinitely long time (as $t \to -\infty$).

Angular size

The angular size for an object with perpendicular diameter D is given by

$$\theta = \frac{D}{R(t_\mathrm{e})\varpi_\mathrm{e}} = \frac{D(1+z)}{\varpi_\mathrm{e}}. \tag{17.6}$$

For the two solutions given above, one finds

$$k = 0,\ \Omega_{\rm M} = 1,\ \Omega_\Lambda = 0 \quad \Rightarrow \quad \theta \ = \ \frac{H_0 D(1+z)}{2c\left(1-\sqrt{1/(1+z)}\right)}, \tag{17.7}$$

$$k = 0,\ \Omega_{\rm M} = 0,\ \Omega_\Lambda = 1 \quad \Rightarrow \quad \theta \ = \ \frac{H_0 D(1+z)}{cz}. \tag{17.8}$$

For local (i.e., z not too large), an expansion in terms of $q_0 = \frac{1}{2}\Omega_{\rm M} - \Omega_\Lambda$ is often more useful. See CO.

Standard candles

The luminosity distance d_L is defined such that

$$F = \frac{L}{4\pi\varpi_{\rm e}^2(1+z)^2} = \frac{L}{4\pi d_L^2} \qquad \Rightarrow \qquad d_L = \varpi_{\rm e}(1+z)\ . \tag{17.9}$$

Again, one can write a local expansion in terms of q_0 (see CO), or find general solutions. For the two cases listed above,

$$k = 0,\ \Omega_{\rm M} = 1,\ \Omega_\Lambda = 0 \quad \Rightarrow \quad d_L \ = \ \frac{2c}{H_0}\left(1+z-\sqrt{1+z}\right) \tag{17.10}$$

$$k = 0,\ \Omega_{\rm M} = 0,\ \Omega_\Lambda = 1 \quad \Rightarrow \quad d_L \ = \ \frac{c}{H_0}(z+z^2). \tag{17.11}$$

This way of measuring cosmological parameters has been applied most successfully, using supernovae of type Ia: see Figs. 17.1, and 17.2. For a review, see Leibundgut (2001, ARA&A 39, 67); for more recent results, see results from the SNLS survey, e.g., Astier et al. (2006, A&A, 447, 31) and Sullivan et al. (2011, ApJ, 737:102).

Note that in general the "dark energy" discussed in §15 (and included above in Ω_Λ) need not be a cosmological constant per se, but something with an exotic "equation of state" which yields a pressure $p_\Lambda = w\rho_\Lambda$, where negative values of w yield acceleration of the expansion of the universe. A cosmological constant is equivalent to $w = -1$ (which is often simply assumed to be the case), but other values of w (possibly varying with time) correspond to other forms for Λ (varying with time). From supernova data, combined with other constraints, Sullivan et al. (2011, ApJ, 737:102) presently infer $w = -1.06 \pm 0.07$, i.e., the data are consistent with a cosmological constant.

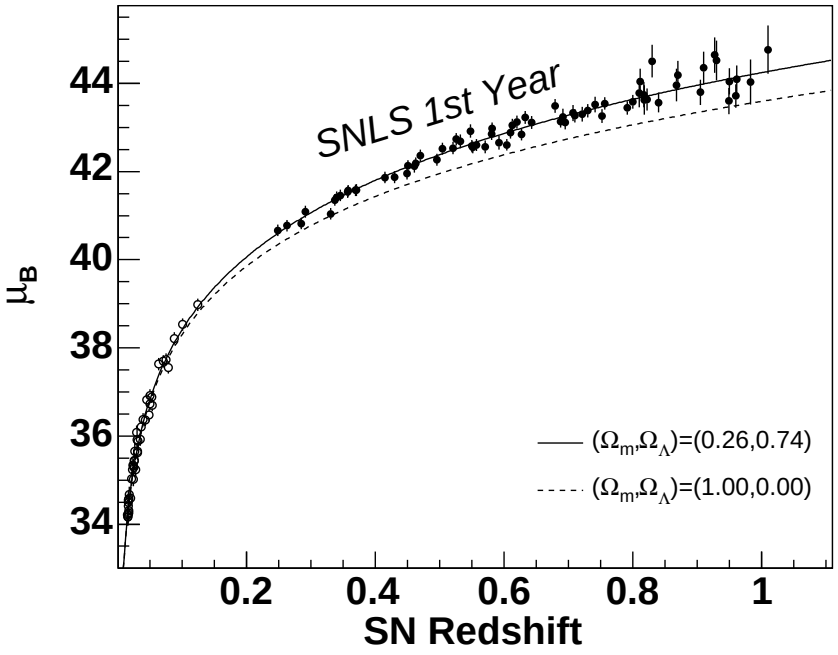

Fig. 17.1. Hubble diagram of type Ia supernovae, taken from Astier et al. (2006, A&A, 447, 31). Lines for two cosmological models are drawn, as labelled.

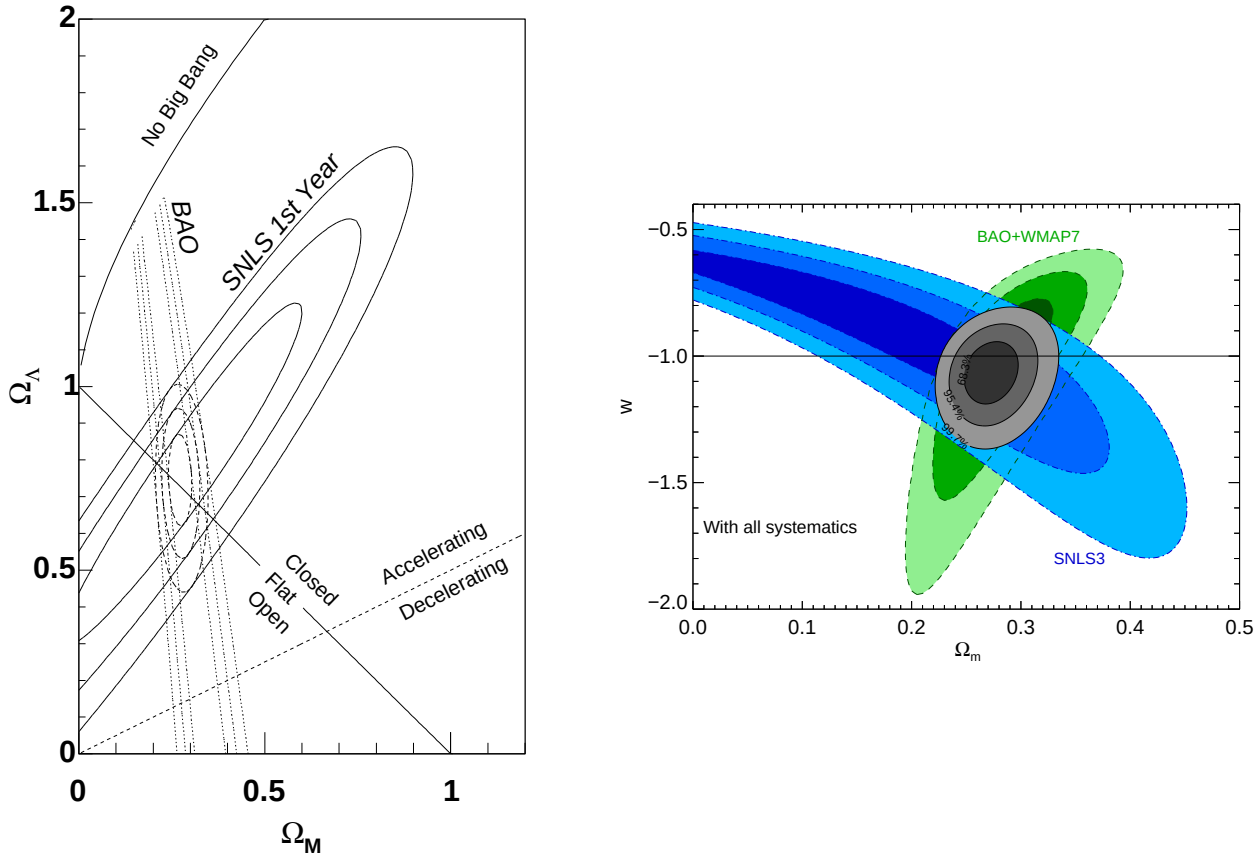

Fig. 17.2. Constraints on Ω_M and Ω_Λ (left) and Ω_Λ and w (right). The probability contours are at the 1, 2, and 3 σ levels. Left panel from Astier et al. (2006, A&A, 447, 31), right one from the three-year update of Sullivan et al. (2011, ApJ, 737:102) .

18. Inflation and the Cosmic Microwave Background (CMB)

Textbook: §28.2, up to p. 1317; §27.2

End of the radiation era

The end of the radiation era occurs when $\rho_{\rm m} = \rho_\gamma$, i.e.,

$$\rho_0(1+z)^3 = \frac{aT_0^4}{c^2}(1+z)^4 \quad \Rightarrow \quad 1+z = \frac{3\Omega_0 H_0^2 c^2}{8\pi G a T_0^4} \simeq 2.2\times 10^4 \Omega_0 \left(\frac{H_0}{75\,{\rm km\,s^{-1}\,Mpc^{-1}}}\right)^2 , \qquad (18.1)$$

where $T_0 = 2.736$ K is the present photon temperature, i.e., the temperature of the cosmic microwave background (CMB) radiation. Including the neutrinos in the energy in relativistic particles at early times, one should change a into $a' = a(1 + \frac{7}{8}N_\nu(T_\nu/T)^4) = 1.68a$, where $N_\nu = 3$ and $T_\nu/T \approx (4/11)^{1/3}$ (neutrinos have a lower temperature because of the extra energy put into the photons when the electrons and positrons annihilated). The current best estimate is that the period when matter and radiation densities were equal occurred at $z \approx 3230 \pm 200$.

Decoupling

Suppose there was no recombination. Consider a flat universe at early enough times that the cosmological constant term can be neglected, i.e., for $R^3 \ll 1$, and thus $t \approx \frac{2}{3}H_0^{-1}\Omega_0^{-1/2}(1+z)^{-3/2}$. Then the optical depth to electron scattering (over $\sim ct$, i.e., of order a horizon size) is

$$\tau_{\rm es} = \sigma_{\rm T} n_{\rm e} ct \approx \sigma_{\rm T}\,\frac{\rho_{\rm B,0}(1+z)^3}{m_{\rm H}}\,\frac{2c(1+z)^{-3/2}}{3H_0\Omega_0^{1/2}} \approx \frac{0.035(1+z)^{3/2}\Omega_{\rm B,0}}{\Omega_0^{1/2}}\left(\frac{H_0}{75\,{\rm km\,s^{-1}\,Mpc^{-1}}}\right) . \qquad (18.2)$$

For $\Omega_{\rm B,0} \approx 0.04$, $\Omega_0 \approx 0.3$, and $H_0 \approx 71\,{\rm km\,s^{-1}\,Mpc^{-1}}$, it follows that the optical depth to electron scattering over a horizon size drops to unity ($\tau_{\rm es} = 1$) at the point $1 + z \simeq 56$. At that point, however, the CMB temperature would be $T \approx 150\,{\rm K}$ and Hydrogen would already have recombined long since.

Recombination

For simplicity, assume pure Hydrogen. Then, from the Saha equation (Eq. 5.9), scaling to $n_{\rm B} = \rho_{\rm B,0}(1+z)^3/m_{\rm H}$, and writing in terms of the ionized fraction $x \equiv n_{\rm p}/n_{\rm B}$,

$$\frac{x^2}{1-x} = \frac{n_p n_e}{n_{H^0} n_{\rm B}} = \frac{m_{\rm H}}{\rho_{\rm B,0}(1+z)^3}\,\frac{(2\pi m_{\rm e} k T_0(1+z))^{3/2}}{h^3}\,{\rm e}^{-\chi/kT_0(1+z)} , \qquad (18.3)$$

where n_{H^0} is the number density of neutral hydrogen. Solving this for $\Omega_{\rm B,0} \approx 0.04$ and $x = 0.5$, gives $1 + z \approx 10^3$. In reality, recombination will be a little delayed as photons produced in the recombination can excite and ionize other atoms: current estimates yield $1 + z \approx 1090$ for the typical redshift at the time a CMB photon last scattered. Moreover, this "surface of last scattering" has a finite thickness $\Delta z \approx 200$.

Reionization

The first generation of luminous stars and/or quasars at $z \sim 20$ produced enough UV radiation to reionize the intergalactic medium. However, the density at this point had become low enough that the optical depth to electron scattering remained small.

Smoothness and flatness problems

Smoothness or *horizon problem*: The CMB radiation is very nearly isotropic (after one corrects for the dipole induced by our relative motion). However, at the time of recombination, the horizon size (in terms of comoving coordinates ϖ) was much smaller than it is now — regions that are now separated by more than a couple of degrees should *never* have been in causal contact before the time when the CMB was forming. How then could they "know" how to have such very similar temperatures and densities (to about a part in 10^5)?

Flatness problem: For some time, it has been known that the present observed density of the universe is close to the critical value (within an order of magnitude), which implies it must have been very close to the critical value at early times. During the era when matter density dominates over radiation density ($\rho = \rho_0/R^3$), we can write the ratio of the density to the critical density as a function of scale factor R, using the Freedmann equation:

$$\Omega \equiv \frac{\rho}{\rho_c} = \frac{8\pi G\rho_0}{3R^3H^2} = \frac{\Omega_0 H_0^2}{R^3H^2} = \frac{\Omega_0 H_0^2}{R^3H_0^2(\Omega_0/R^3 + \Omega_{\Lambda,0} - kc^2/R^2)} = \frac{1}{1 + R^3\frac{\Omega_{\Lambda,0}}{\Omega_0} + R\frac{\Omega_{k,0}}{\Omega_0}} \ , \qquad (18.4)$$

where Ω_0, $\Omega_{\Lambda,0}$, and $\Omega_{k,0} = -kc^2/H_0^2$ are present values as in section 16. But this suggests that there ought to be some reason why the universe was so very close to flat at early times.

Inflation

Both of the above problems can be solved by invoking "inflation". At present, we have a good theory describing how, at high enough energies, the weak force and the electromagnetic force are "unified" into the electroweak force (i.e., they can no longer be distinguished at higher energies). A similar unification between the electroweak force and the strong force is expected in a grand unified theory (GUT), at a much higher energy (see CO Fig. 28.7, p. 1310), though the theories are not quite as well developed. As the temperature in the early universe drops, this GUT energy scale is encountered, and one would expect the symmetry between the strong and electroweak forces to be broken. However, under some conditions, this symmetry breaking would not occur immediately: the universe (or some portion thereof) could enter a metastable "supercooled" state, where the temperature was lower than the GUT unification scale but the phase transition from GUT symmetry to separate strong and electroweak forces had not yet taken place. This state behaves as if there is a *very* strong cosmological constant (driven by the scalar field connected with the GUT symmetry breaking), and the size of (that portion of) the universe grows exponentially with time, on a very short timescale — this is known as "inflation". The energy density also approaches exponentially close to the critical density: this fixes the *flatness problem*.

Due to inflation, a causally connected region is rapidly stretched by many orders of magnitude; even the present horizon size sees only a tiny fraction of this original causally-connected region. Thus, wherever you look on the sky, what you see originated essentially in the same place as any other patch of the sky, so it is not surprising that it looks the same: this fixes the *smoothness problem*. The rapid inflation dilutes any original particle density essentially to zero, but when the GUT phase transition occurs (dropping from the metastable state to the ground state), the energy of this transition "reheats" the universe, generating copious amounts of photons and particle–anti-particle pairs. GUT theories inply a slight asymmetry between particles and anti-particles, so at the later time when the photon energy drops below twice the particles' rest energy (and the particles annihilate with antiparticles without being regenerated) there is a small excess of particles left over.

Inflation also blows up the scale of quantum fluctuations in the scalar field that drives inflation and eventually the re-heating. Thus inflation predicts stochastic fluctions of the temperature, density, and gravitational potential that have a particular form. Since the exponential expansion is self-similar in time, these fluctuations are scale-invariant, i.e., in each logarithmic interval in scale the contribution to the variance of the fluctuations is equal. (Note that often one considers the power

spectrum, i.e., the square of the amplitudes of the fluctuations.) Such fluctuations are essentially 'frozen in' as long as they are larger than the horizon.

After inflation has ended, the horizon size again starts to grow (in terms of comoving coordinates). As fluctuations of larger and larger size become encompassed by the horizon, they start to evolve. For example, cold dark matter (CDM) interacts only very weakly, and thus has essentially no pressure. In overdense region it will thus tend to collapse, due to self-gravitation; this appears to be the original source of much of the observed structure in the universe, at least of galactic scale and larger. Ordinary matter likewise tends to collapse into the gravitational potential produced (largely) by the cold dark matter, eventually yielding galaxies inside halos of cold dark matter. Note that smaller-sized fluctuations start to collapse first, since they are the first to become encompassed by the growing horizon: galaxies and clusters tend to grow through mergers of smaller structures.

Cosmic Microwave Background Radiation

After recombination, the cosmic microwave background (CMB) radiation streams essentially freely through space from the "surface of last scattering" described above. It therefore preserves essentially unchanged the effects of the temperature and density fluctuations that existed *at that time*.

Fluctuations in the microwave background are generally presented in terms of coefficients C_ℓ for fluctuations of a given angular size on the sky — for (Gaussian) temperature fluctuations as a function of position on the sky $\Delta T/T = \Theta(\theta, \phi)$, the multipole moments of the CMB temperature

$$\Theta_{\ell m} = \int \sin\theta \mathrm{d}\theta \mathrm{d}\phi \, Y^*_{\ell m} \, \Theta(\theta, \phi) \tag{18.5}$$

are fully characterized by their power spectrum

$$\langle \Theta^*_{\ell m} \Theta_{\ell' m'} \rangle = \delta_{\ell\ell'} \delta_{mm'} C_\ell \ . \tag{18.6}$$

Note that a given wavelength on the sky θ corresponds to $2\pi/\ell$. The power spectrum is frequently presented in terms of

$$\Delta^2_T \equiv \frac{\ell(\ell+1)}{2\pi} \, C_\ell \, T^2 \tag{18.7}$$

(which for $\ell \gg 1$ is the power per logarithmic interval in wavenumber k).

Cosmic variance

Note that the C_ℓ are measurements of the *variance* of the CMB fluctuations, a statistical quantity whose accuracy is limited by sample size. For a given ℓ value, the range of m values is $-\ell \le m \le \ell$, thus there are only $(2\ell + 1)$ samples at a given ℓ. This implies an inevitable error due to "cosmic variance" of

$$\Delta C_\ell = \sqrt{\frac{2}{2\ell+1}} \, C_\ell \ . \tag{18.8}$$

(Since one cannot use the entire sky, because of foreground emission in and near the galactic plane, this error is increased slightly.) There is no way we can determine any monopole term ($\ell = 0$), nor can a dipole term be distinguished from the dipole that results from our motion relative to the CMB frame, and other low-ℓ terms have large uncertainties. On the other hand, at higher ℓ one can bin the data, averaging over ℓ in bands of size $\Delta\ell \propto \ell$, in order to obtain final uncertainties at a given ℓ that are of order ℓ^{-1} (provided there are no other sources of uncertainty). Fig. 18.1 shows the first-year results from *Planck*. The origin of the peaks at large ℓ (small angular size) are discussed further below.

Large scales are an unchanged record of inflation

Relatively large-scale fluctuations (more than a couple of degrees across on the sky, as noted above), were larger than the horizon size at the time of recombination. Thus they underwent no evolution prior to the recombination era, retaining the scale-invariant form left behind by inflation.

The fluctuations from inflation can be described as small deviations in the (Newtonian) gravitational potential Ψ. These yield small deviations in how fast time ran: $\delta t/t = \Psi$. The scale factor R depends on t: when radiation dominates, $R \propto t^{1/2}$, and when matter dominates $R \propto t^{2/3}$. Of course, we also have $T \propto R^{-1}$ for the cosmic background radiation (from Eq. 14.7). As noted above, recombination occurs after the end of the radiation-dominated era; thus we may describe the intrinsic temperature fluctuations as

$$\Theta \equiv \left(\frac{\delta T}{T}\right)_{\rm intrinsic} = -\frac{\delta R}{R} = -\frac{2}{3}\,\frac{\delta t}{t} = -\frac{2}{3}\,\Psi\ . \tag{18.9}$$

However, at recombination, the photons have to climb out of the gravitational potential Ψ (Sachs-Wolfe effect), and thus are red-shifted accordingly (or blue-shifted, if the region is underdense). What we actually see on the sky is thus

$$\Theta_{\rm obs} \equiv \left(\frac{\delta T}{T}\right)_{\rm obs} = \left(\frac{\delta T}{T}\right)_{\rm i} + \Psi = \Theta + \Psi = \frac{1}{3}\,\Psi\ , \tag{18.10}$$

i.e., the *underdense* regions at recombination on the sky are observed to be brighter than the intrinsically-hotter overdense regions, since the radiation has been blue-shifted to higher temperature in the former case and red-shifted in the latter.

Smaller scales evolved, yielding peaks in CMB power spectrum

Evolution of the 'frozen-in' fluctuations actually occurs when the relevant region is in causal contact in the hydrodynamic sense, i.e., within the **"sound horizon"**, the distance

$$s = \int_0^t c_s\,\frac{{\rm d}t'}{R(t')}\ , \qquad \text{where} \quad c_s = \sqrt{\frac{\partial P}{\partial \rho}} = \sqrt{\frac{\partial \frac{1}{3}\,aT^4}{\partial\, aT^4/c^c}} = \frac{c}{\sqrt{3}} \tag{18.11}$$

is the sound speed in the radiation-dominated era. In this approximation, it can be shown that the balance between radiation pressure and gravity yields an equilibrium at

$$\Theta + \Psi = \frac{\Delta T}{T} + \Psi = 0\ . \tag{18.12}$$

However, the initial temperature fluctuations are just the intrinsic ones described above, namely $\Theta = -\frac{2}{3}\Psi$. Thus, in the absence of damping, the evolution of temperature at any point will be an oscillation as a function of time around the equilibrium value, i.e., $-\frac{2}{3}\Psi \le \Theta \le -\frac{4}{3}\Psi$, yielding $-\frac{1}{3}\Psi \le \Theta_{\rm obs} \le \frac{1}{3}\Psi$ at recombination depending on the phase of the oscillation at that point.

Since all fluctuations of a given angular size enter the horizon at the same time, they all start evolving in phase. Small regions will evolve faster due to having shorter sound travel timescales (as well as beginning to evolve earlier). Large regions will have time to go through only a small fraction of an oscillation cycle before recombination, and will be somewhat reduced in amplitude. However, a somewhat smaller region, of such a size that it has time to go through half an oscillation cycle, will regain its original amplitude (though of opposite sign, i.e., an overdensity is converted into an underdensity, and vice versa); this yields a peak in the power spectrum at the corresponding ℓ value. The next peak in the power spectrum results from regions that regain their original amplitude by going through a full oscillation cycle: see Fig. 18.2, part (a). Thus the existence of peaks on the CMB power spectrum is a generic prediction of the inflationary paradigm.

The above idealized description requires some modification, however. There is damping of the oscillations: for the smaller sizes, photons can diffuse into and out of the relevant regions, smearing out the fluctuations. Consequently, the CMB power spectrum drops off at higher ℓ values, as may be seen in Fig. 18.1, and more clearly in Fig. 18.3 (which extends to higher ℓ).

The presence of baryons shifts the zero-point of the oscillations downwards, to

$$\Theta + (1+\mathcal{R})\Psi = \frac{\Delta T}{T} + (1+\mathcal{R})\Psi = 0 \ , \qquad \text{where} \quad \mathcal{R} = \frac{p_{\rm B}/c + \rho_{\rm B}}{p_\gamma/c + \rho_\gamma} \ , \tag{18.13}$$

i.e., $\mathcal{R}$ is the baryon momentum density ratio; thus the first, third, fifth, etc. peaks should have larger amplitudes than the second, fourth, sixth, etc. peaks, as may be seen from Fig. 18.2, part (b). Baryons also reduce the sound speed to $c_s = c/\sqrt{3(1+\mathcal{R})}$. The actual effect of baryons on the CMB power spectrum is shown in Fig. 18.3, part (c); the above alternate-peak effect is superimposed on the overall decline in power with increasing ℓ.

The position of the peaks depends on the curvature of the universe. In a closed universe, the circumference of a circle is less than 2π times its radius; thus, at a fixed coordinate distance, a given angular scale corresponds to a smaller spatial scale. Thus the acoustic peaks would appear at larger angles (smaller ℓ) for a closed universe $\Omega_{\rm tot} > 1$, and conversely at smaller angles (larger ℓ) for an open universe $\Omega_{\rm tot} < 1$. This sensitivity to curvature is shown (for $0.1 \leq \Omega_{\rm tot} \leq 1$) in Fig. 18.3, part (a). On the other hand, the CMB power spectrum is not very sensitive to dark energy (a cosmological constant), as is shown in Fig. 18.3, part (b).

In essence, cold dark matter particles are coupled with photons, baryons, and other cold dark matter particles only by gravity, and exert no pressure. Thus the presence of cold dark matter reduces the oscillations, and therefore also the amplitudes of the peaks in the CMB power spectrum, as shown in Fig. 18.3, part (d).

Estimation of Cosmic Parameters

The CMB power spectrum can be used to estimate various cosmological parameters, as shown in Fig. 18.4, which gives the cosmological parameters extracted from the results of *Planck*, as well as those data combined with results from other cosmological probes (which yields even tighter constraints)

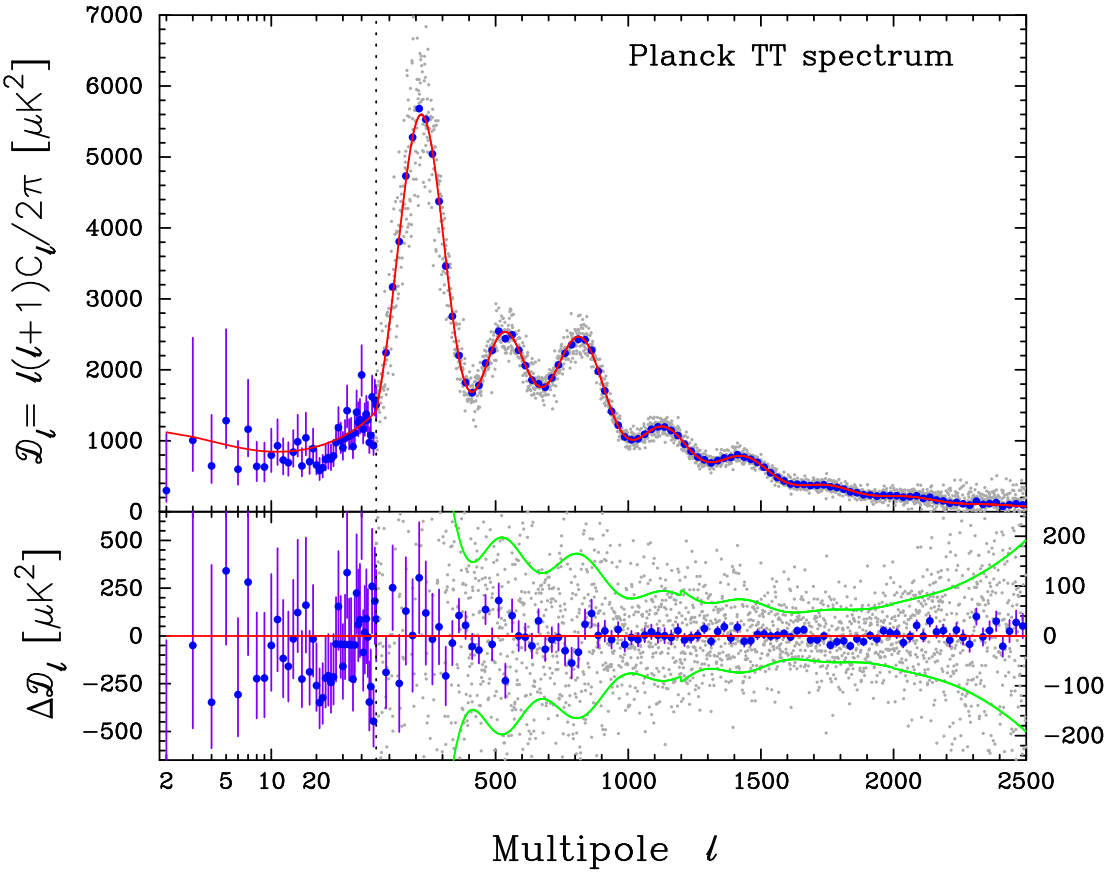

Fig. 18.1. Temperature fluctuations in the CMB as measured by the Planck collaboration (2013, arXiv:1303.5067), showing both the binned data (solid points with error bars, from combined measurement and cosmic variance errors), and the unbinned data (gray points).

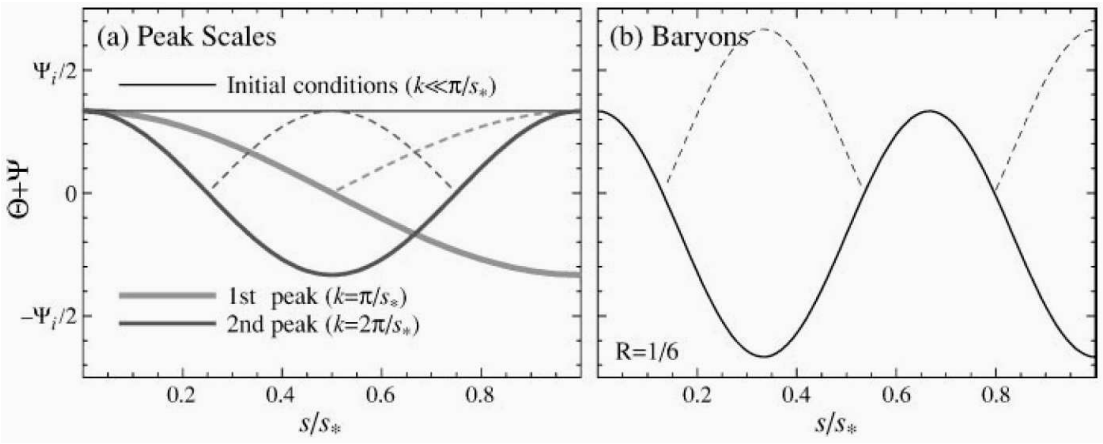

Fig. 18.2. From Hu & Dodelson (2002), ARAA, 40, 171: Idealized acoustic oscillations, with time measured in terms of the extent s of the sound horizon relative to its extent s_* at recombination. (a) *Peak scales*: the wavemode that completes half an oscillation by recombination sets the physical scale of the first peak in the CMB power spectrum. Both maxima and minima in $\Theta + \Psi$ correspond to peaks in power (*dashed lines* give the absolute value of the amplitude), so subsequent peaks in the CMB power spectrum would be at integral multiples of this scale, with equal amplitude in this idealized case. (b) *Baryon loading*: the presence of baryons reduces the sound speed and also changes the zero point of the oscillation, thus boosting the amplitude of alternate peaks. Plotted here is an idealization of a case for the third peak, with baryon momentum density ratio $R \equiv \mathcal{R} = (p_B + \rho_B)/(p_\gamma + \rho_\gamma) = 1/6$, in units where the speed of light $c = 1$ (note that in this figure R is *not* the scale factor of the universe).

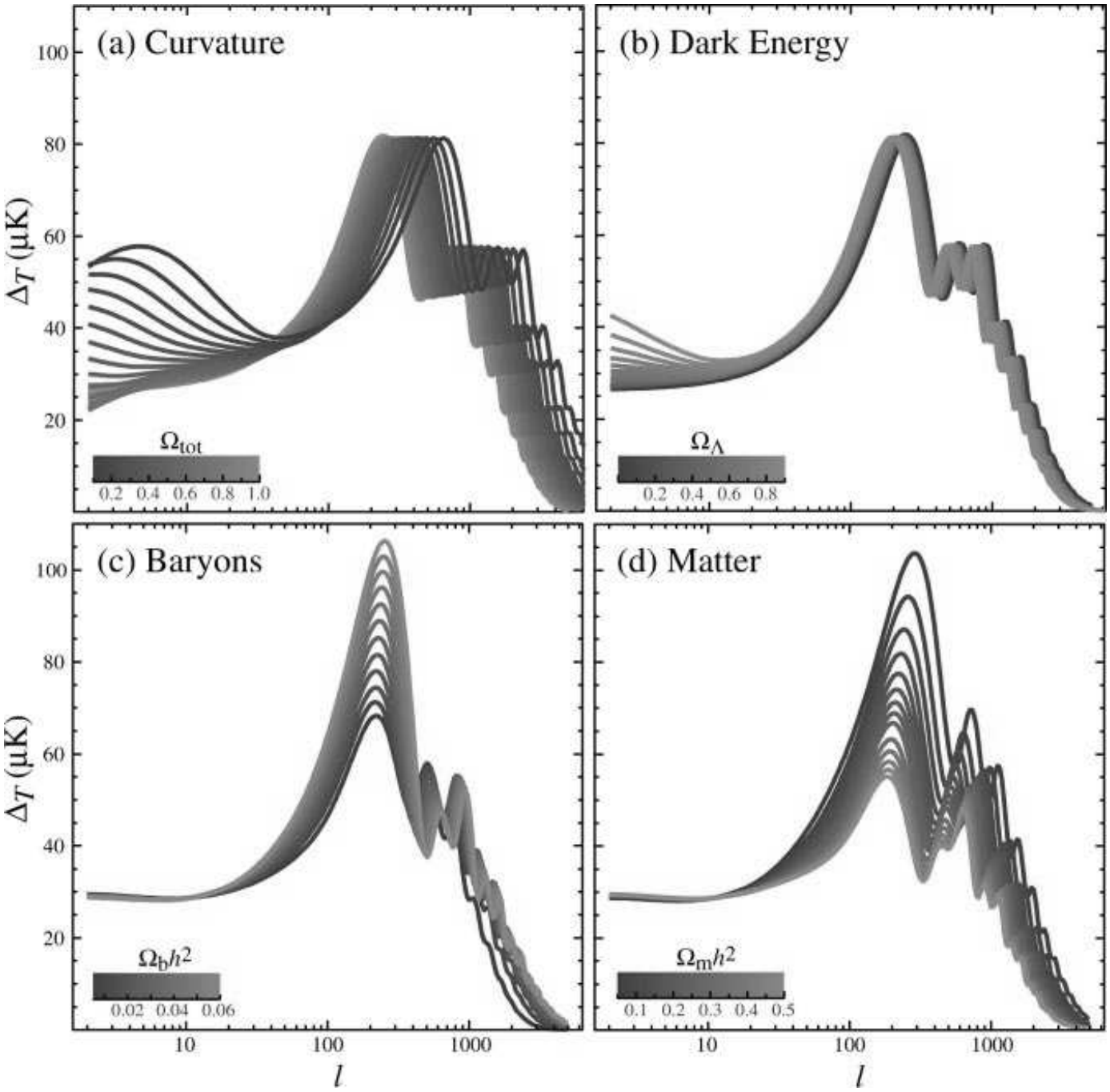

Fig. 18.3. From Hu & Dodelson (2002), ARAA, 40, 171: Sensitivity of the acoustic CMB temperature spectrum to four fundamental cosmological parameters. (a) The curvature, as quantified by $\Omega_{\rm tot}$. (b) The dark energy, as quantified by the cosmological constant Ω_Λ (i.e., dark energy equation of state with $w = -1$). (c) The physical baryon density $\Omega_b h^2$, where $\Omega_b \equiv \Omega_{\rm B}$ and $h \equiv H_0/(100\,{\rm km\,s^{-1}\,Mpc^{-1}})$. (d) The physical matter density $\Omega_m h^2$, where $\Omega_m \equiv \Omega_0$. All are varied around a fiducial model of $\Omega_{\rm tot} = 1$, $\Omega_\Lambda = 0.65$, $\Omega_b h^2 = 0.02$, and $\Omega_m h^2 = 0.147$, with spectral index $n = 1$.

Parameter	*Planck*+WP		*Planck*+WP+highL		*Planck*+lensing+WP+highL		*Planck*+WP+highL+BAO	
	Best fit	68% limits	Best fit	68% limits	Best fit	68% limits	Best fit	68% limits
$\Omega_b h^2$	0.022032	0.02205 ± 0.00028	0.022069	0.02207 ± 0.00027	0.022199	0.02218 ± 0.00026	0.022161	0.02214 ± 0.00024
$\Omega_c h^2$	0.12038	0.1199 ± 0.0027	0.12025	0.1198 ± 0.0026	0.11847	0.1186 ± 0.0022	0.11889	0.1187 ± 0.0017
$100\theta_{MC}$	1.04119	1.04131 ± 0.00063	1.04130	1.04132 ± 0.00063	1.04146	1.04144 ± 0.00061	1.04148	1.04147 ± 0.00056
τ	0.0925	$0.089^{+0.012}_{-0.014}$	0.0927	$0.091^{+0.013}_{-0.014}$	0.0943	$0.090^{+0.013}_{-0.014}$	0.0952	0.092 ± 0.013
n_s	0.9619	0.9603 ± 0.0073	0.9582	0.9585 ± 0.0070	0.9624	0.9614 ± 0.0063	0.9611	0.9608 ± 0.0054
$\ln(10^{10} A_s)$	3.0980	$3.089^{+0.024}_{-0.027}$	3.0959	3.090 ± 0.025	3.0947	3.087 ± 0.024	3.0973	3.091 ± 0.025
A_{100}^{PS}	152	171 ± 60	209	212 ± 50	204	213 ± 50	204	212 ± 50
A_{143}^{PS}	63.3	54 ± 10	72.6	73 ± 8	72.2	72 ± 8	71.8	72.4 ± 8.0
A_{217}^{PS}	117.0	107^{+20}_{-10}	59.5	59 ± 10	60.2	58 ± 10	59.4	59 ± 10
A_{143}^{CIB}	0.0	< 10.7	3.57	3.24 ± 0.83	3.25	3.24 ± 0.83	3.30	3.25 ± 0.83
A_{217}^{CIB}	27.2	29^{+6}_{-9}	53.9	49.6 ± 5.0	52.3	50.0 ± 4.9	53.0	49.7 ± 5.0
A_{143}^{tSZ}	6.80	...	5.17	$2.54^{+1.1}_{-1.9}$	4.64	$2.51^{+1.2}_{-1.8}$	4.86	$2.54^{+1.2}_{-1.8}$
$r_{143\times217}^{PS}$	0.916	> 0.850	0.825	$0.823^{+0.069}_{-0.077}$	0.814	0.825 ± 0.071	0.824	0.823 ± 0.070
$r_{143\times217}^{CIB}$	0.406	0.42 ± 0.22	1.0000	> 0.930	1.0000	> 0.928	1.0000	> 0.930
γ^{CIB}	0.601	$0.53^{+0.13}_{-0.12}$	0.674	0.638 ± 0.081	0.656	0.643 ± 0.080	0.667	0.639 ± 0.081
$\xi^{tSZ\times CIB}$	0.03	...	0.000	< 0.409	0.000	< 0.389	0.000	< 0.410
A^{kSZ}	0.9	...	0.89	$5.34^{+2.8}_{-1.9}$	1.14	$4.74^{+2.6}_{-2.1}$	1.58	$5.34^{+2.8}_{-2.0}$
Ω_Λ	0.6817	$0.685^{+0.018}_{-0.016}$	0.6830	$0.685^{+0.017}_{-0.016}$	0.6939	0.693 ± 0.013	0.6914	0.692 ± 0.010
σ_8	0.8347	0.829 ± 0.012	0.8322	0.828 ± 0.012	0.8271	0.8233 ± 0.0097	0.8288	0.826 ± 0.012
z_{re}	11.37	11.1 ± 1.1	11.38	11.1 ± 1.1	11.42	11.1 ± 1.1	11.52	11.3 ± 1.1
H_0	67.04	67.3 ± 1.2	67.15	67.3 ± 1.2	67.94	67.9 ± 1.0	67.77	67.80 ± 0.77
Age/Gyr	13.8242	13.817 ± 0.048	13.8170	13.813 ± 0.047	13.7914	13.794 ± 0.044	13.7965	13.798 ± 0.037
$100\theta_*$	1.04136	1.04147 ± 0.00062	1.04146	1.04148 ± 0.00062	1.04161	1.04159 ± 0.00060	1.04163	1.04162 ± 0.00056
r_{drag}	147.36	147.49 ± 0.59	147.35	147.47 ± 0.59	147.68	147.67 ± 0.50	147.611	147.68 ± 0.45

Fig. 18.4. Cosmological parameters from *Planck* (Planck collaboration, arXiv:1303.5076; their Table 5), both from CMB alone (left) and including other cosmological constraints.